

3. Stellar Coronae

GOALS FOR THE APPLICATION OF HIGH-RESOLUTION X-RAY
SPECTROSCOPY TO THE DIAGNOSIS OF STELLAR CORONAL PLASMAS

Jeffrey L. Linsky*

Joint Institute for Laboratory Astrophysics
University of Colorado and National Institute of Standards
and Technology, Boulder, CO, USA

Don Quixote - The mission of each true knight...
his duty - nay, his privilege!
To dream the impossible dream,

...
To reach the unreachable star,
Though you know it's impossibly high,
To live with your heart striving upward,
To a far, unattainable sky!

(Man of La Mancha - Wasserman et al. (1966))

ABSTRACT

I provide examples of how high-resolution x-ray spectra may be used to determine the temperature and emission measure distributions, electron densities, steady and transient flow velocities, and location of active regions in stellar coronae. For each type of measurement I estimate the minimum spectral resolution required to resolve the most useful spectral features. In general, high sensitivity is required to obtain sufficient signal-to-noise to exploit the high spectral resolution. Although difficult, each measurement should be achievable with the instrumentation proposed for AXAF.

1. PERSPECTIVE

May I share with you my nearly impossible dream in the hope that its description will speed its fulfillment within our "scientific" lifetimes. I dream that we will extend the powerful diagnostic techniques for ultraviolet and optical spectra, which are now used to infer the properties of astrophysical plasmas at $\log T = 3.5-5.2$, to the x-ray domain where hot coronal plasmas ($\log T = 6-8$) emit the bulk of their radiation. The fulfillment of this dream requires the combination of high sensitivity and spectral resolution that will become feasible with AXAF and with later missions like XMM. As I shall describe in some detail, the scientific results can be enormous, although some experiments will push technology to its limits.

*Staff Member, Quantum Physics Division, National Institute of Standards and Technology

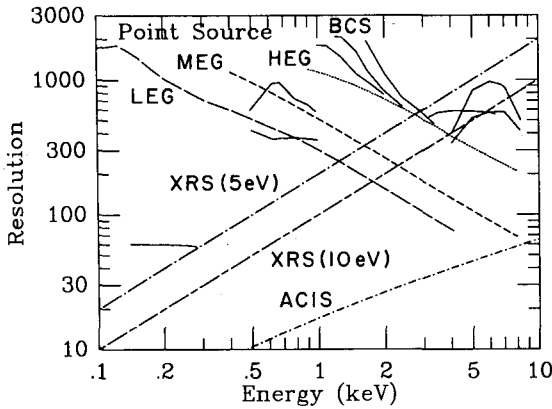


Figure 1. Anticipated resolving power $R = E/\Delta E$ of the AXAF spectrometers for point sources. The acronyms for the individual instruments are defined in the text. The solid lines refer to different crystals in the BCS. The resolving power of the XRS is given for assumed energy resolutions of 5 eV and 10 eV.

AXAF's spectrometers and detectors have not yet been fully developed, but we can anticipate what their final capabilities should be if no insurmountable difficulties are encountered. The six AXAF spectroscopic instruments (the Bragg Crystal Spectrometer - BCS, Low Energy Transmission Grating Spectrometer - LEG, Medium Energy Grating - MEG, High Energy Grating - HEG, X-ray Spectrometer (Microcalorimeter) - XRS, and Advanced CCD Imaging Spectrometer - ACIS) are described in papers presented at a special session of the AAS in January 1986 (Canizares *et al.* 1987; Brinkman *et al.* 1987; Holt 1987; and Nousek *et al.* 1987). The anticipated capabilities of these instruments are still evolving, and I am indebted to Claude Canizares and Tom Markert for providing the current compilation of the anticipated resolving power (Figure 1) and effective area (Figure 2) as a function of energy for these instruments.

In this talk I shall concentrate on the advantages of the high spectral resolution of AXAF, although the satellite will also have excellent high-throughput imaging capabilities. The high spectral resolution capabilities of XMM and other future missions are not yet determined and will not be discussed further. The scientific objectives that I shall shortly describe require high spectral resolution with a

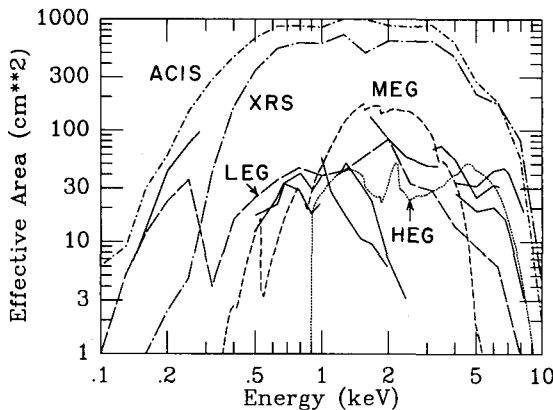


Figure 2. Anticipated effective areas for the AXAF spectrometers. The acronyms for the individual instruments are defined in the text. The solid lines refer to different crystals in the BCS.

resolving power $R = E/\Delta E > 500$. By this criterion the high-resolution instruments are the LEG ($E < 0.5$ keV), MEG ($E = 0.4-0.8$ keV), HEG ($E = 0.9-2.2$ keV), BCS ($E = 0.95-1.9$ and $3-8$ keV), and the XRS ($E > 2.5$ keV), assuming that the XRS will achieve an energy resolution of 5 eV). Thus high resolution spectroscopy is feasible over the full spectral range of AXAF if all of the above instruments are confirmed and perform as anticipated. Better still, $R > 1000$ should be achieved in limited spectral intervals ($E < 0.2$ keV, $1-2$ keV and > 5 keV), and $R \sim 2000$ may be achieved near 0.1 keV and near 1 keV.

High resolution without high sensitivity has limited utility. The effective area plots in Figure 2 show that $A_{\text{eff}} > 10$ cm² for at least one of the high-resolution ($R > 500$) spectrometers over nearly the full energy range. In addition, $A_{\text{eff}}(\text{MEG}) = 100$ cm² near 1 keV and $A_{\text{eff}}(\text{ACIS}) = 1000$ cm² between 2.5 and 4 keV where $R > 500$. Thus high-throughput, high-sensitivity spectroscopy appears to be feasible over limited spectral intervals. By comparison, the Einstein SSS had $R = 7$ and $A_{\text{eff}} = 100$ cm² at 1 keV and the 500 line/mm transmission grating had $R = 50$ and $A_{\text{eff}} = 1$ cm² over its useful energy range (Giacconi *et al.* 1979). While the crystals in the BCS have $A_{\text{eff}} = 30-100$ cm² over much of their energy range, the spectral interval observed at any one time is small, so that the values of A_{eff} must be divided by the number of energy bins to be scanned in order to compare the BCS with other instruments that are spectrally multiplexed.

I shall now quantify the required high sensitivity needed to take advantage of high spectral resolution. A useful study of this question is provided in a paper by Landman, Roussel-Dupre and Tanigawa (1982). They computed the statistical uncertainties in the amplitude (A), line-center wavelength (B), and Doppler width (C) in a least-squares fit of an observed spectral line by a Gaussian

$$y(x) = A \exp\{-[(x-B)/C]^2\}, \quad (1)$$

where $y(x)$ is the flux at a given wavelength x . They showed that for normally distributed errors in which the noise is independent of x , the uncertainties in the measured values of A, B and C are given by

$$S_A/A, S_B/C, S_C/C \propto (S/N)^{-1} (dx/C)^{1/2}, \quad (2)$$

where dx is the spectral resolution and the S/N ratio is measured at line center using the signal per dx interval. Thus to measure the line shift and width to, say, 10% requires at least 100 counts per resolution element, provided the spectral line is resolved ($dx < C$). Conversely, low S/N data provide very uncertain values for all three Gaussian fit parameters even when the line is resolved.

To estimate whether the AXAF high-resolution spectrometers can obtain a sufficient number of counts in important spectral lines of bright coronal sources, the effective area of the AXAF instruments must be multiplied by the computed flux for the assumed stellar emission

measure distribution. Several plasma emission codes exist, such as those of Mewe and Gronenschild (1981), Doschek and Cowan (1984), Shull (1986), and Raymond and Smith (1977).

Doschek and Cowan (1984) have computed the photon rates at Earth between 10\AA ($E = 1.24\text{ keV}$) and 200\AA ($E = 0.062\text{ keV}$) for two bright RS CVn systems (Capella and UX Ari) using approximations to their emission measure distributions derived by Swank *et al.* (1981) from Einstein SSS data. Two of their simulated spectra for Capella with an instrumental resolution of 0.25\AA (R increases from 40 to 300 in the wavelength interval) are shown in Figure 3. The counts per 0.25\AA bin are for a 10 second integration when $A_{\text{eff}} = 40\text{ cm}^2$. Thus an integration time of only one minute is sufficient to provide >100 counts for the brighter lines in these spectral regions, indicating that the sensitivity is sufficient to take advantage of high resolution spectroscopy. The spectral resolution of $R = 40\text{-}300$ in this simulation is inadequate, however, because a great many of the apparently single emission lines are blends as indicated by comparison with the higher resolution emission rate spectra (see Figure 3). Their simulated spectra of the important Fe XXIV 192.0\AA line at different resolutions shows that $R = 800$ is needed to resolve this line. The value of $R = 800$ may be typical of what is required, although the resolution required to resolve specific lines must be determined on a case by case basis.

Another example of the sensitivity of the AXAF spectroscopic instruments is Linsky's (1987) computation of the total line counts in 1000 seconds for the 17 brightest lines (or close blends) between 10\AA and 14\AA using the Doschek and Cowan (1984) plasma emissivities and the Swank *et al.* (1981) emission measure distribution for another RS CVn system -- V711 Tau (=HR 1099). The numbers of counts in 1000 seconds lie in the range 20-620 for observations with the MEG and 60-1700 for observations with the XRS. The number of counts for the BCS should be roughly 1/4 that of the MEG if the lines have FWHM=300 km/s and the BCS steps through the line profiles. Several hundred counts per line are feasible in only 100 seconds for the brightest line (FeXX 12.82\AA) observed with the XRS, but 40,000 seconds are required for the faintest of the 17 lines (NeIX 11.56\AA) observed with the BCS. Thus many lines are bright enough to effectively utilize high-resolution spectroscopy.

The sensitivity and spectral resolution of the AXAF instruments, as well as the spectrometers that may fly on XMM and Spektrosat, far exceed the capabilities of the Einstein and Exosat spectrometers, previously described by Schmitt and Pallavicini.

2. APPLICATION OF SPECTROSCOPIC DIAGNOSTICS TO THE MEASUREMENT OF THE THERMODYNAMIC PROPERTIES OF STELLAR CORONAL PLASMAS

The availability of high-resolution spectra of the quiet and flaring Sun obtained with the P78-1, SMM and Hinotori spacecraft and with laboratory sources has stimulated the development of diagnostics to measure the temperature, emission measure distribution, electron

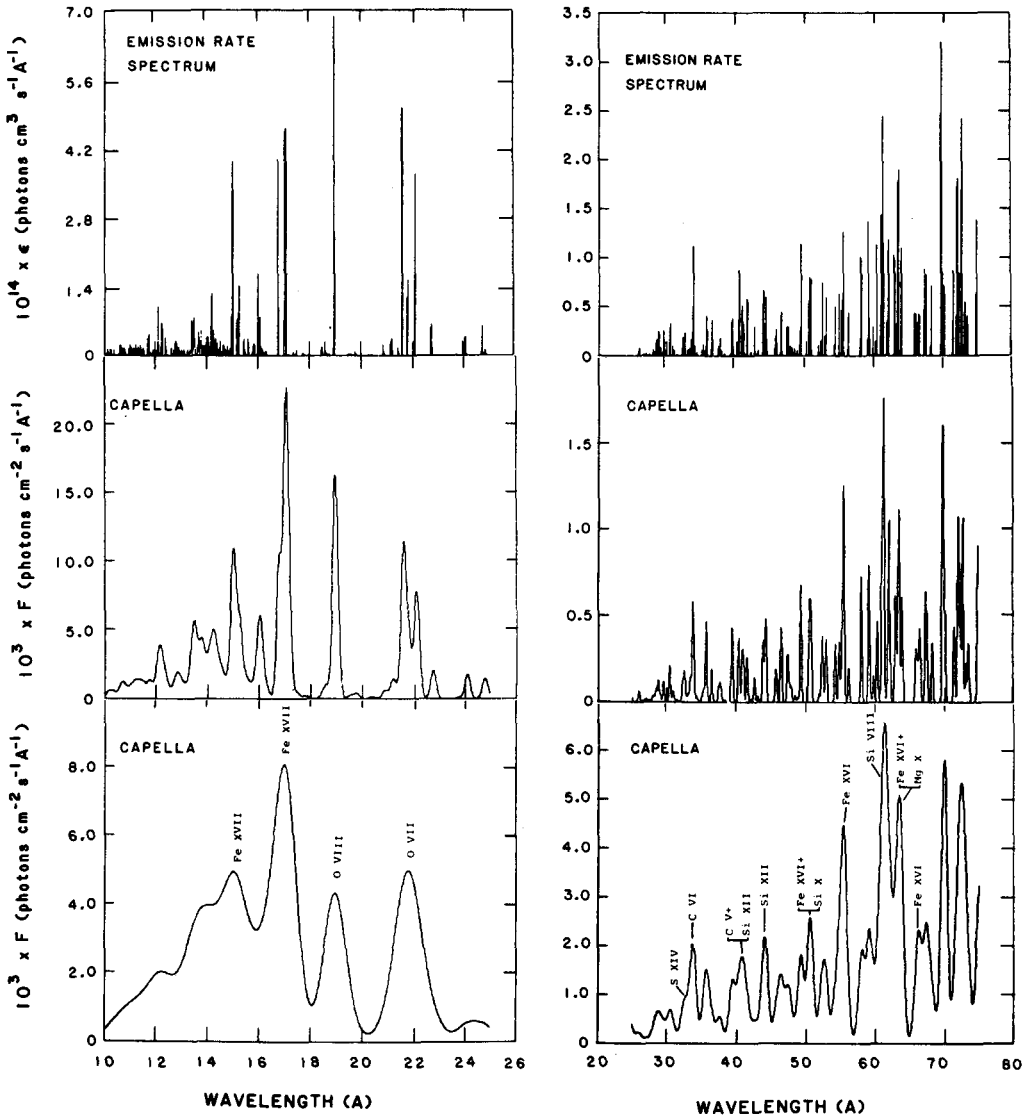


Figure 3. Emission rate spectra (fluxes per unit emission measure, instrumental resolution 0.02Å) for two wavelength regions are compared with simulated spectra for Capella with instrumental resolutions of 0.25Å (middle plots) and 1Å (lower plots). (From Doschek and Cowan 1984.)

density, and departures from coronal ionization equilibrium. Space does not permit a comprehensive review of this large topic, and I shall emphasize a few important diagnostics which provide critical tests of the spectral resolution and sensitivity required for the proper diagnosis of stellar coronal plasmas. I direct the reader to Mason's review in these Proceedings as well as to the reviews by Feldman (1981), Dere and Mason (1981), and Dupree (1978).

2.1 Temperature and Emission Measure Diagnostics

The first evidence that stellar coronal plasmas are not isothermal was provided by the SSS low resolution ($\Delta E = 140$ eV) spectra of seven RS CVn systems and Algol that Swank *et al.* (1981) showed should be fit by at least two-temperature plasmas, with the emission measure, EM(T), peaked near $\log T = 6.8$ and $7.5-8.0$. The SSS spectrum of the M dwarf system Wolf 630 AB ($dM3.5e+dM3.5e$) has also been fit with a two-temperature plasma with peaks in the EM(T) at $\log T = 6.8$ and >7 (Swank and Johnson 1982). In their study of EXOSAT transmission grating spectra of two RS CVn systems (Capella and σ^2 CrB), Lemen *et al.* (1988) concluded that both spectra are better fit by an EM(T) distribution peaked near $\log T = 6.7$ and 7.5 than by a continuous distribution. The Mewe *et al.* (1982) analysis of the Einstein Objective Grating Spectrometer (R= 15-75) spectrum of Capella also results in a two-temperature fit with $\log T = 6.7$ for the cooler component but $\log T = 7.0$ for the hotter component. The analyses of moderate resolution spectra of the RS CVn systems are thus in close agreement except for the less well determined hotter component.

Majer *et al.* (1986), however, fit the much lower resolution IPC spectra of seven RS CVn systems in common with the SSS data set also with two-temperature plasmas, but in all cases both the cool and hot components have derived temperatures a factor of 3 lower. While the analysis of higher resolution data must be given greater weight, discrepancies among the conclusions of different authors, the absence of a compelling argument for thermal bifurcation, and the absence of steady-state plasma in either temperature range in the solar corona suggest that the two-temperature distributions may provide an incomplete picture of the plasma properties in stellar coronae. The only way to settle this question is to obtain and analyze higher-resolution spectra with good signal-to-noise. This last point is important, because the Einstein Bragg Crystal spectra of Capella have a resolution $R \sim 150$ but sufficient sensitivity to detect only three lines (O VIII 18.97\AA , Fe XVII 15.01\AA , and FeXX 12.83\AA) in 60,000 seconds observing. Vedder and Canizares (1983) were able to derive from these data a mean temperature ($\log T = 6.8$) for the plasma but no information on the temperature distribution.

A simple method for deriving the temperature of an assumed isothermal coronal plasma is to compare the observed fluxes in collisionally-excited lines of different ions of the same element with flux ratios computed assuming coronal steady-state ionization and excitation equilibrium. A virtue of this method is that spectral lines

may be selected on the basis of their strength and absence from obvious blends. Since the ionization ratio technique can use the brightest and least blended among a large number of possible lines, the simulated spectra in Figure 3 suggest that $R = 200$ may be sufficient to find enough suitable lines, although higher resolution would be desirable. This method is limited, however, by inaccurate atomic data and uncertain assumptions underlying the ionization equilibrium calculations. Even worse, such calculations assume the unlikely physical situation that the plasma is homogeneous and isothermal, that the electron velocity distribution is maxwellian without a high energy tail, that the ionization is steady state and in balance with the local electron temperature and density, and that photoionization is unimportant. The ionization equilibrium in the outer solar corona is frozen-in, however, since the time scale for the wind to transport plasma to regions of significantly different temperature and density exceeds the time scale for ionization and recombination (Owocki, Holzer, and Hundhausen 1983). Also, transient ionization occurs in flares (Doschek and Tanaka 1987), and flaring may be responsible for the bulk of coronal heating. Even when the standard coronal ionization equilibrium assumptions are valid, the temperatures at which specific ions have peak abundance often differs by $\Delta \log T = 0.1$ among different calculations as a result of different assumed ionization and recombination rates.

Uncertainties in the ionization equilibrium may be avoided by measuring the flux of two spectral lines of the same ion for which their ratio is sensitive to temperature rather than density. This occurs, for example, when both lines are collisionally excited from the ground state (or a common lower level) and de-excitation is radiative rather than collisional. Their flux ratio for an isothermal plasma will only depend upon atomic cross-sections and the Boltzmann factor, $\exp[-(E_2 - E_1)/kT_e]$, where E_1 and E_2 are the excitation energies of the two upper levels relative to the lower state. One particularly useful ratio is $F(3p-3s)/F(3d-3p)$ of the NaI isoelectronic sequence (including FeXVI 251Å/263Å), because the two lines are close in wavelength (cf. Flower and Nussbaumer 1975) and thus instrumental flux calibration uncertainties should be minimal. Additional line ratios are summarized in the previously listed reviews. The spectral resolution required is set by the need to avoid significant blends and is, therefore, different for each line pair. A typical resolution needed for medium strength lines is about $R = 800$ as shown in the Doschek and Cowan (1984) simulated spectra of the region near the important FeXXIV 192.0Å line.

A third method for inferring plasma temperatures uses the ratio of line fluxes within the K shell transition blend of He-like ions such as CaXIX (3.18-3.20Å) and FeXXV (1.85-1.87Å). The $F(j)/F(w)$ ratio is particularly important, because the fluxes of both the dielectronic satellite line (j) and the collisionally-excited resonance line (w) depend upon the population of the He-like ion. Thus the ratio depends upon the electron temperature (T_e) rather than the electron density or ionization equilibrium. On the other hand, the $F(q)/F(w)$ ratio can be used to measure departures from coronal ionization equilibrium, because line q is an inner-shell collisional excitation line of the Li-like ion,

whereas line *w* is the collisionally-excited resonance line of the He-like ion. For a more complete discussion of the atomic physics of these transitions and applications to the diagnosis of solar coronal plasmas see, for example, Feldman (1981). The important point of this discussion is that the typical splitting of lines in the CaXIX 3.19Å region is 0.0040Å and in the FeXXV 1.86Å region is 0.0024Å. Thus $R = 800$ is required to diagnose both regions. Both the BCS and the XRS (for an energy resolution $\Delta E = 8$ eV) have sufficient resolution at 1.86Å (6.6 keV), but only the XRS (for $\Delta E = 5$ eV) has sufficient resolution at 3.19Å (4.0 keV). The anticipated effective area of the XRS at 4.0 keV is 700 cm² compared with 200 cm² at 6.6 keV and 25 cm² per resolution element for the BCS at this energy. Thus the XRS would be the instrument of choice and the Ca XIX feature the appropriate temperature diagnostic if the XRS can achieve the required resolution $\Delta E = 5$ eV.

2.2 Electron Density Diagnostics

The determination of EM(T) alone is inadequate to model a stellar corona because the unknown density or pressure means that the emitting volume and its geometry are unknown, and the plasma may not be homogeneous or in hydrostatic equilibrium. These two approximations are very unlikely if magnetic loops control the geometry and confine high density structures as occurs in the solar corona. Thus one needs density-sensitive diagnostics that cover the important temperature range to constrain the models. Ratios of lines for a given ion are density sensitive when the radiative de-excitation rates for two transitions to the same lower level are very different. Thus, over a range of density de-excitation transitions are predominately radiative in one transition but predominately collisional in the other.

One can understand the essential physics of the line ratio method by considering an ion with a ground state (1) and two excited states (2 and 3) which are, for illustrative purposes, only connected to the ground state. If we assume that the lines are optically thin and radiative excitation is unimportant, then the statistical equilibrium equation for each excited state is

$$n_u(A_{u1} + n_e C_{u1}) = n_1 n_e C_{1u} \quad (3)$$

and the emergent flux in each transition is

$$F_{u1} = A_{u1} h\nu n_u. \quad (4)$$

The line flux ratio, $r = F_{21}/F_{31}$, is then

$$r = (A_{21}/A_{31}) * [n_e C_{12}/(A_{21} + n_e C_{21})] / [n_e C_{13}/(A_{31} + n_e C_{31})]. \quad (5)$$

This ratio will be density sensitive within some density range when the radiative de-excitation rate for one transition is much larger than for the other. A good example is the BeI isoelectronic sequence ion CIII (cf. Keenan *et al.* 1984) for which the optically allowed ($2s2p \ ^1P - 2s^2 \ ^1S$) 977Å resonance line has a spontaneous de-excitation rate $A_{31} = 1.7$

10^9 s^{-1} , whereas the 1908Å intersystem transition ($2s2p \ ^3P_0 - 2s^2 \ ^1S$) has a rate $A_{21}=190 \text{ s}^{-1}$. In the low density ("coronal") limit ($A_{21}>n_e C_{21}$ and $A_{31}>n_e C_{31}$), the line flux ratio is simply $r=C_{12}/C_{13}$, which is independent of density. In this limit the fluxes of both lines are proportional to the emission measure and thus behave as "allowed" lines. On the other hand, in the high density limit ($A_{21}<n_e C_{21}$ and $A_{31}<n_e C_{31}$), the line flux ratio is also a constant, because both transitions are collisionally de-excited and behave as "forbidden" transitions. The interesting regime occurs at intermediate densities when $A_{21}<n_e C_{21}$ but $A_{31}>n_e C_{31}$. Now the line flux ratio depends explicitly on n_e ,

$$r = A_{21}C_{12}/n_e C_{21}C_{13} \sim 1/n_e. \quad (6)$$

One can define a critical density, $n_e(\text{cr}) = A_{21}/C_{21}$ which is a practical upper limit to the density for which r is a useful density diagnostic.

A number of useful line ratios for FeXVIII-XXVI and other highly ionized species are available in the x-ray region as described in Feldman's (1981) review, although collisional and radiative transitions among excited levels often result in a more complex situation than the simple case just described. Of particular importance are the HeI sequence ions for which Gabriel and Jordan (1969) showed that ratios of the forbidden ($1s^2 \ ^1S_0 - 1s2s \ ^3S_1$) to the intercombination ($1s^2 \ ^1S_0 - 1s2p \ ^3P_1$) lines are density sensitive. The important ratios for the HeI sequence are listed in Table 1 with data from Pradhan and Shull (1981). Included in the table are the wavelengths, temperatures (T_m) at which each ion has maximum abundance, and range of electron densities over which the line ratio is density sensitive. The OVII lines are routinely used as density diagnostics for solar flares, and the lines of CV through NeIX should be useful for studying stellar coronae and flares.

Table 1. Density-Sensitive Line Ratios

Ion	Isoelectronic Sequence	Line Wavelengths (Å)	Transition	$\log(T_m)$	Useful Range in $\log(n_e)$	Ref.
C V	He I	40.73/41.47	$1S_0 - ^3S_1 / ^1S_0 - ^3P_1$	5.5	> 8.8	1
O VII	He I	21.80/22.02	"	5.9	>10.5	1
Ne IX	He I	13.55/13.70	"	6.2	>11.8	1
Mg XI	He I	9.23/9.32	"	6.4	>12.7	1
Si XIII	He I	6.69/6.74	"	6.6	>13.6	1
Ca XIX	He I	3.19/3.21	"	7.4	>15.4	1
Fe XXV	He I	1.86/1.87	"	7.7	>16.8	1
Fe XXII	B I	114.41/117.18	$2P_3^0/2 - ^2P_3/2 / ^2P_1^0/2 - ^2S_1/2$	7.0	12-14	2
Fe XXII	B I	11.93/11.74	$2P_3^0/2 - ^2D_3/2, 5/2 / ^2P_1^0/2 - ^2D_3/2$	7.0	12-14	2
Fe XXI	C I	142.14/128.74	$3P_1 - ^3D_2 / ^3P_0 - ^3D_1$	7.0	11-13	3
Fe XXI	C I	102.35/128.74	$2P_2 - ^3S_1 / ^3P_0 - ^3D_1$	7.0	11-13	3
Fe XXI	C I	12.38/12.313	$3P_2 - ^3D_3 / ^3P_0 - ^3D_1$	7.0	11-13	3

References: (1) Pradhan and Shull (1981); (2) Mason and Storey (1980); (3) Mason *et al.* (1979).

Since the separation of these lines increases from $E/\Delta E = 60$ for CV to 90 for NeIX, a modest resolution of $R = 150$ would be adequate. The higher ions in the sequence are unlikely to be useful as their critical densities are very large. Some line ratios of FeXXI and FeXXII used for analyzing solar flares are listed in Table 1.

3. APPLICATION OF SPECTROSCOPIC DIAGNOSTICS TO THE MEASUREMENT OF THE FLOWS AND GEOMETRY OF STELLAR CORONAL PLASMAS

3.1 Winds and Downflows

Is it feasible to measure the expansion velocities of stellar coronae with high-resolution x-ray spectroscopic techniques? To answer this question we must understand the dynamics and geometry of stellar coronae. Since we know very little about these properties in stellar coronae, it is useful to start with the Sun. The solar wind passing the Earth ranges in velocity from roughly 400 km/s up to 800 km/s in high speed streams. The steady-state mass loss rate at the equator is roughly $2 \times 10^{-14} M_{\odot}/\text{yr}$ with some 5-10% of the total occurring in sudden ejections of material in the form of coronal mass ejections (CMEs) which are in part flare related. At present no spectroscopic indicator of mass loss is apparent in the spectrum of the Sun viewed as an unresolved star. In fact, the only spectroscopic evidence of expanding hot plasma comes from the measurements of the OV 629Å and MgX 625Å lines by Orrall, Rottman and Klimchuk (1983) and previous experimenters. They measured a mean blueshift of about 8 km/s in the MgX line, which is formed at $\log(T) = 6.15$, above a coronal hole, but redshifts of this line in the surrounding active region. In general, these and previous studies found an anticorrelation between the flow direction and line intensity consistent with the picture of upflows in low-density, magnetically-open structures (coronal holes) and downflows in high-density, magnetically-closed regions (active regions). The upflow velocities are far smaller than the terminal velocity of the solar wind, because the MgX line is formed low in the corona where the density is much larger than at the critical point. If the Sun were observed as a point source, even this small velocity would be difficult to detect given the redshifts of the much brighter active regions.

The solar example does not provide optimism for the detection of coronal winds, but the solar mass loss rate is as much as eight orders of magnitude smaller than that measured in some luminous cool stars. In her recent review of mass loss from cool stars, Dupree (1986) summarized the spectroscopic evidence for outflowing material from cool giants and supergiants, pre-main sequence stars, and hybrid chromosphere stars. These data consist of blue-shifted absorption features or P Cygni-shaped profiles of lines formed only at relatively low temperatures, including MgII, CaII, HI, HeI, and neutral atoms formed in circumstellar envelopes. Outflow velocities approaching 200 km/s have been detected in the hybrid star α TrA (Hartmann *et al.* 1985) and in the G1b-II star 22 Vul (Reimers and Che-Bohnenstengel 1986), but the higher temperature lines of CIII and SiIII in an IUE spectrum of α TrA (Brown *et al.* 1986)

show no significant blueshifts, indicating that the hotter material does not participate in the outflow. For the more active stars including the RS CVn binaries, main sequence stars, and the G2 Ib-IIa star β Dra, high-resolution IUE spectra of lines formed at $\log(T) = 4.0 - 5.0$ exhibit a trend of increasing red shift (downflow) with temperature of formation. Mariska (1988) explains these data by asymmetric heating in magnetic loops that produces steeper temperature gradients and thus less emission measure for the upflowing plasma than for the downflowing plasma. Thus, the net spectrum of a star covered with such loops would show redshifted lines, even though there is no net flow of material. These calculations predict that lines formed at $\log(T) > 5.3$ will be blueshifted rather than redshifted, and x-ray spectra are needed to test this prediction. The maximum redshifts for ultraviolet emission lines measured by Ayres *et al.* (1988) in active stars like Capella are about 20 km/s.

Could either winds or downflows in coronae be detected with x-ray spectroscopy? Using Eq. (2) with an assumed line width $C = 150$ km/s and $S/N = 10$, I find that a resolution $R = 1000$ is sufficient to measure line shifts as small as 20 km/s. This quantity scales as $R^{1/2}/(S/N)$. Thus only modest spectral resolution and S/N are required to measure x-ray lineshifts comparable with the ultraviolet results. However, the determination of flow properties in stellar coronae and how they relate to the flow pattern lower in a stellar atmosphere requires considerable theoretical analysis.

3.2 Transient Flows

Blueshifted components in coronal emission lines are commonly seen during the early stages of solar flares. These components detected in the CaXIX 3.176Å line have been interpreted by Antonucci *et al.* (1984, 1987) and others as indicating 10^7 K plasma upflows with velocities as large as 400 km/s at the impulsive stage of a flare decreasing to essentially zero in 3-10 minutes near the peak of the thermal x-ray emission. A common interpretation of this phenomenon is that nonthermal electrons accelerated during the impulsive event heat and evaporate the chromosphere at the footpoints of magnetic loops, producing the rapid expansion of 10^7 K plasma up the loops. These upflows have never been detected in stellar flares. Flows during flares on RS CVn stars are detected in chromospheric lines like H α and MgII k, but the line shifts and additional components are generally to the red indicating downflows (e.g. Simon *et al.* 1980; Linsky *et al.* 1988).

How are these flows related to the solar flare evaporative flows detected in x-rays, and do evaporative flows also occur during stellar flares? Since the spectroscopic signature of the upflows is the presence of blueshifted components adjacent to the main emission line, a resolution of 200 km/s ($R = 1500$) is required and $R = 3000$ is desirable. In addition, a time resolution of 5 minutes or better is needed if the solar example is pertinent. These requirements are stringent but can be met with the AXAF LETGS. Linsky (1987) estimates that the LETGS will obtain 84 counts in 5 minutes in the FeXVI 63.71Å line for a flare

similar to that observed from AT Mic (dM4.5e+dM4.5e) by Kahn et al. (1979).

3.3 Doppler Imaging

The presence of bright or dark structures on the surfaces and above the limbs of stars can be detected by timing and spectroscopic techniques. The presence of dark spots on the photospheres of active stars, for example, is indicated by photometric variations with the stellar rotational period. Similarly, the presence of discrete, bright active regions in stellar chromospheres is indicated by the increase and decrease in emission line flux as an active region appears and then disappears over the limb. The correlation of photometric decline with MgII and CIV flux increase and the reverse behavior half a rotational period later led Rodono et al. (1987) to conclude that during October 1981 a bright active region was located above a large spot complex on the RS CVn star II Peg.

Photometric and spectrophotometric techniques provide only crude data on the location of spots and active regions on a star. A more precise technique is Doppler imaging which analyzes the changing Doppler shift of a discrete region on a rapidly-rotating star as the region rotates across the stellar disk to determine both its longitude and latitude (from the amplitude of the radial velocity changes). Vogt and Penrod (1983) and Vogt et al. (1987) have developed this technique to obtain images of RS CVn systems with several dark spot groups. Walter et al. (1987) and Neff et al. (1988) have used these techniques to locate two or three bright active regions in the chromosphere of the KO IV star of their favorite RS CVn-type system AR Lac.

Can the Doppler imaging technique be applied to x-ray spectra to derive images of stellar coronae? This is a very demanding task as the equatorial rotational velocities of these systems are generally less than 70 km/s and most active dwarf stars rotate more slowly. To test the feasibility of this technique, we plot in Figure 4 profiles of the NeX 12.20Å line from the KO IV star in AR Lac ($v \sin i = 72$ km/s) assuming that half the flux is from a structure with a Doppler shift of 100, 200, and 300 km/s relative to the star for assumed resolving powers $R = 1000, 2000$ and 3000 . The Doppler shifts are for a corotating structure located in the equatorial corona 0.4, 1.8, and 3.2 stellar radii above the limb. These calculations indicate that with good S/N and a stable wavelength scale a resolution of only 1000 is required to identify the closest structure, but a resolution of 3000 would locate the active region reliably and permit its study as a function of phase. Thus the goal of Doppler imaging of stellar coronae is probably not an impossible dream.

4. CONCLUSIONS

Each type of measurement described in this paper places different requirements on the instrumental spectral resolution. In some cases

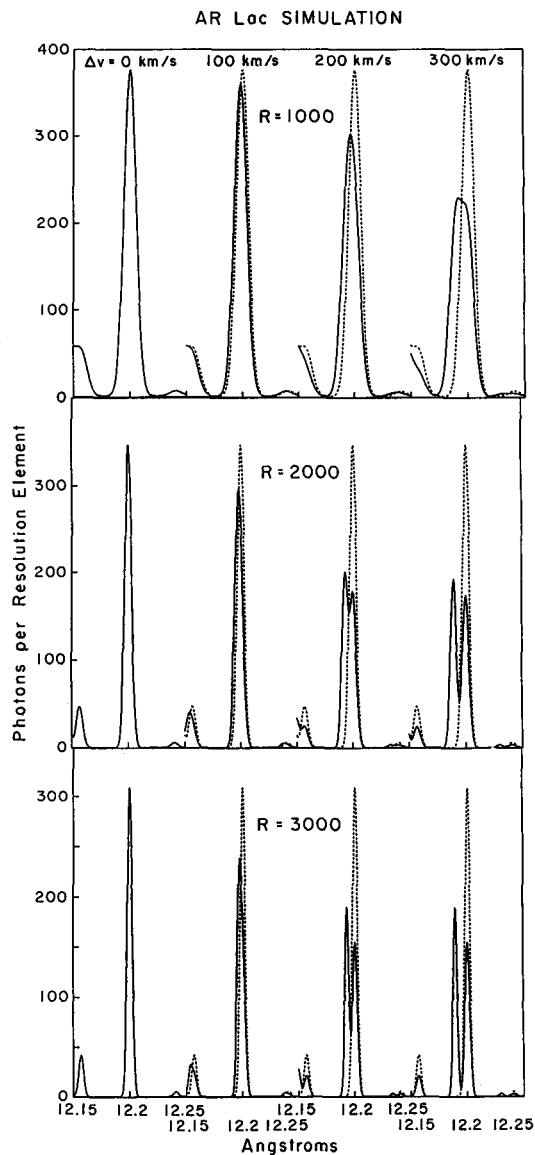


Figure 4. Simulated profiles of the NeX 12.20Å line from the KO IV star in AR Lac. Each line profile is a convolution of 20 km/s turbulence, 72 km/s rotation, and an instrumental resolution $R = 1000$ (top panel), 2000 (middle panel), or 3000 (bottom panel). Half of the emission is from the stellar disk and half from an active region with a Doppler shift of $\Delta v = 0, 100, 200,$ or 300 km/s towards the observer. The dashed profiles are for $\Delta v = 0$ km/s to compare with the profiles including a Doppler-shifted active region. The calculation assumes emission measures from Swank *et al.* (1981) and $A_{\text{eff}}\Delta t = 1 \times 10^6 \text{ cm}^2 \text{ s}$, where A_{eff} is the instrumental effective area and Δt the integration time. Other lines are present at 12.16 and 12.24Å.

Table 2. Summary of Spectral Resolution Requirements

Measurement	Minimum Resolution Required ($R=E/\Delta E$)	Desirable Resolution
Measure coronal temperature by the ionization ratio technique	200	400
Measure coronal temperature from line ratios for a given ion	800	800
Measure coronal temperature and departures from coronal ionization equilibrium using the Ca XIX 3.18-3.02Å or Fe XXV 1.85-1.87Å features	800	1200
Measure electron densities from He sequence ions	150	400
Measure flow velocity of 20 km/s when $S/N=10$	1000	1000
Measure transient upflows during flares	1500	3000
Doppler image active regions in the coronae of RS CVn systems	1000	3000

there are also preferred spectral regions. Table 2 summarizes the minimum resolutions required for each of the measurements. For most measurements, $R = 1000$ should provide usable information for at least some stellar coronae, although higher resolution is desirable and high signal-to-noise is mandatory. Although difficult, each measurement should be achievable for at least a few stars with the instrumentation proposed for AXAF.

I wish to thank Drs. C. Canizares and T. Markert for providing Figures 1 and 2, and Drs. G. A. Doschek and R. D. Cowan for allowing my use of Figure 3. I also thank Mr. A. Veale for computing the Doppler-imaged profiles in Figure 4. This work is supported by NASA grant H-80531 to NIST.

5. REFERENCES

- Antonucci, E., Gabriel, A. H., and Dennis, B. R. 1984, *Ap. J.*, 287, 917.
 Antonucci, E., Doderer, M. A., Peres, G., Serio, S., and Rosner, R. 1987, *Ap. J.*, 322, 522.
 Ayres, T. R., Jensen, E., and Engvold, O. 1988, *Ap. J. Suppl.*, 66, 51.
 Brinkman, A. C., van Rooijen, J. J., Bleeker, J. A. M., Dijkstra, J. H., Heise, J., De Korte, P. A. J., Mewe, R., and Paerels, F. 1987, *Astro. Lett. Comm.*, 26, 73.
 Brown, A., Reimers, D., and Linsky, J. L. 1986, *New Insights in Astrophysics*, ESA SP-263, 169.
 Canizares, C. R., *et al.* 1987, *Astro. Lett. Comm.*, 26, 87.
 Dere, K. P. and Mason, H. 1981, in "Solar Active Regions", ed. F. Q. Orrall (Boulder: Colorado Assoc. Univ. Press), p. 129.
 Doschek, G. A. and Cowan, R. D. 1984, *Ap. J. Suppl.*, 56, 67.
 Doschek, G. A. and Tanaka, K. 1987, *Ap. J.*, 323, 799.
 Dupree, A. K. 1978, *Adv. Atomic Mol. Phys.*, 14, 393.

- Dupree, A. K. 1986, Ann. Rev. Astron. Ap., 24, 377.
- Feldman, U. 1981, Physica Scripta, 24, 681.
- Flower, D. R. and Nussbaumer, H. 1975, Astron. Ap., 42, 265.
- Gabriel, A. H. and Jordan, C. 1969, M.N.R.A.S., 145, 241.
- Giacconi, R. et al. 1979, Ap. J., 230, 540.
- Hartmann, L., Jordan, C., Brown, A., and Dupree, A. K. 1985, Ap. J., 296, 576.
- Holt, S. S. 1987, Astro. Lett. Comm., 26, 61.
- Kahn, S. M., Linsky, J. L., Mason, K. O., Haisch, B. M., Bowyer, C. S., White, N. E., and Pravdo, S. H. 1979, Ap. J., 234, L107.
- Keenan, F. P., Berrington, K. A., Burke, P. G., Kingston, A. E., and Dufton, P. L. 1984, M.N.R.A.S. 207, 459.
- Landman, D. A., Roussel-Dupre, R., and Tanigawa, G. 1982, Ap. J., 261, 732.
- Lemen, J. R., Mewe, R., Schrijver, C. J., and Fludra, A. 1988, Ap. J., submitted.
- Linsky, J. L. 1987, Astro. Lett. Comm., 26, 21.
- Linsky, J. L., Neff, J. E., Brown, A., Gross, B. D., Simon, T., Andrews, A. D., Rodono, M., and Feldman, P. A. 1988, Astron. Ap., in press.
- Majer, P., Schmitt, J. H. N. N., Golub, L., Harnden, F. R. Jr., and Rosner, R., 1986, Ap. J., 300, 360.
- Mariska, J. T. 1988, Ap. J., 334, 489.
- Mason, H. E., Doschek, G. A., Feldman, U., and Bhatia, A. K. 1979, Astron. Ap., 73, 74.
- Mason, H. E. and Storey, P. J. 1980, M.N.R.A.S. 191, 631.
- Mewe, R. and Gronenschild, E. H. B. M. 1981, Astron. Ap. Suppl., 45, 11.
- Mewe, R., et al. 1982, Ap. J. 260, 233.
- Neff, J. E., Walter, F. M., Rodono, M., and Linsky, J. L. 1988, Astron. Ap., in press.
- Nousek, J. A., Garmire, G. P., Ricker, G. R., Collins, S. A., and Reigler, G. R. 1987, Astro. Lett. Comm., 26, 35.
- Orrall, F. Q., Rottman, G. J., and Klimchuk, J. A. 1983, Ap. J., 266, L65.
- Owocki, S. P., Holzer, T. E., and Hundhausen, A. J. 1983, Ap. J., 275, 354.
- Pradhan, A. K., and Shull, J. M. 1981, Ap. J., 249, 821.
- Raymond, J. C., and Smith, B. W. 1977, Ap. J. Suppl., 35, 419.
- Reimers, D., and Che-Bohnenstengel, A. 1986, Astron. Ap., 166, 252.
- Rodono, M., et al. 1987, Astron. Ap., 176, 267.
- Shull, J. M. 1986, private communication.
- Simon, T., Linsky, J. L., and Schiffer, F. H. III 1980, Ap. J., 239, 911.
- Swank, J. H., White, N. E., Holt, S. S., and Becker, R. H. 1981, Ap. J., 246, 208.
- Swank, J. H., and Johnson, H. M. 1982, Ap. J., 259, L67.
- Vedder, P. W., and Canizares, C. R. 1983, Ap. J., 270, 666.
- Vogt, S. S. and Penrod, G. D. 1983, Publ. Astron. Soc. Pacific, 95, 565.
- Vogt, S. S., Penrod, G. D., and Hatzes, A. P. 1987, Ap. J., 321, 496.
- Walter, F. M., Neff, J. E., Gibson, D. M., Linsky, J. L., Rodono, M., Gary, D. E., and Butler, C. J. 1987, Astron. Ap., 186, 241.
- Wasserman, D., Darion, M., and Leigh, M. 1966, "Man of La Mancha" (New York: Random House).

DISCUSSION-J. Linsky

S. Serio: You did mention non-ionization equilibrium. Where can it be observed in stellar coronae? In fact, SMM does not see NIE in solar flares because higher sensitivity would be needed.

J. Linsky: We should look for departure from coronal ionization equilibrium during stellar flares by whatever diagnostics are available. One such diagnostic is the $F(q)/F(w)$ ratio of the inner-shell collisional excitation line of the Li-like ion to the collisionally-excited resonance line of the He-like ion. These lines are located near 3.9 Å for C₆ and 1.86 Å for Fe.

R. Pallavicini: Just to give the proper credit to the authors, I have to say that the comparison of x-ray temperatures derived from IPC and SSS observations is due to the work of P. Majer, J. Schmitt and Collaborators (Ap.J. 1986), and not to me.

The second comment I have is that high-resolution spectroscopy will also help understanding the physics of early-type stars, with regard to both line broadenings (as expected from turbulent winds) and Doppler shifts due to wind expansion.

J. Linsky: I agree with both of your comments.

S. Kahn: 1) Do the Spectral predictions for UX Ari and Capella include interstellar absorption out at 19Å ? and 2) Many of your suggested "experiments" push the instrumental limits. Do you think there are an equal number of exciting projects for coronae which are a little less demanding?

J. Linsky: 1) The calculated spectra I showed for Capella and UX Ari do not include interstellar absorption. For Capella the hydrogen column density is about $2 \times 10^{18} \text{ cm}^{-2}$, which corresponds to interstellar optical depth unity at about 280 Å and interstellar optical depth about 0.3 at 190 Å. I do not know what the interstellar hydrogen column density is towards UX Ari. 2) While I have concentrated on the more demanding spectroscopic studies, there are important studies that can be made with lower spectral resolution data. For example, with a spectral resolution $E/\Delta E = 10-100$ and large effective area, comparison of observed with theoretical spectra should lead to far more accurate distributions of emission measure with temperature than could be obtained with the Einstein SSS or the EXOSAT TGS. Such data could be obtained for a wide variety of stars, and binary systems, for example, with high time resolution or the brighter transient sources.